Electron-Injection-Assisted Generation of Oxygen Vacancies in Monoclinic HfO_2

Samuel R. Bradley and Alexander L. Shluger
Department of Physics and Astronomy, University College London, Gower Street, London WC1E 6BT, United Kingdom

Gennadi Bersuker
The Aerospace Corporation, Los Angeles, California 90009-2957, USA
(Received 2 September 2015; published 23 December 2015)

Understanding the mechanisms of generation of oxygen vacancies in monoclinic (m)-HfO_2 is important for improving and controlling its performance as an oxide layer in transistor gate stacks and in resistive random-access memory (RRAM) devices. We use *ab initio* calculations to investigate the mechanism of formation of Frenkel pairs of oxygen vacancies and interstitial ions in m-HfO_2 under electron-injection conditions. The results demonstrate that the formation of stable pairs of neutral oxygen vacancies and interstitial oxygen ions assisted by extra electrons is thermodynamically feasible and requires overcoming activation barriers of less than 1.3 eV at preexisting O vacancies. A preexisting oxygen vacancy can act as an electron trap and facilitate the formation of an O vacancy and O interstitial ion pair nearby. The resulting O divacancy is stabilized by weak attraction between neutral vacancies, further lowering the formation energy of the defect pair. The binding energy per vacancy in larger oxygen-vacancy aggregates increases as the aggregate grows, facilitating the formation of defect pairs next to larger vacancy aggregates. These results are useful for understanding the mechanisms of oxide degradation and electroforming in RRAM cells, which can proceed through creation of new O vacancies in the vicinity of preexisting vacancies complementing vacancy aggregation via diffusion processes.

DOI: 10.1103/PhysRevApplied.4.064008

I. INTRODUCTION

Dielectric films control electric fields and carrier distributions in the active regions of electronic devices, such as transistors (in their metal-oxide-semiconductor gate-stack structures) and determine the performance of capacitors and memories. The reliability of such devices is strongly affected by the parasitic electron transport through the film [1–3]. Such transport can self-accelerate leading to further degradation of dielectric and eventually to its breakdown [4–9]. Monoclinic (m)-HfO_2 stands out among many binary oxides employed or investigated as transistor gate dielectrics and materials in the resistive nonvolatile memories (RRAMs) due to demonstrated exceptionally good characteristics and mature process technology [10]. Degradation processes caused by electron transport during device operation in HfO_2 stacks are thought to be caused by both preexisting and newly generated defects, such as oxygen vacancies (see, e.g., Refs. [10–12] and references therein). In particular, electroforming operation in the HfO_2-based RRAM cells has been studied extensively [13–17] and has been shown to lead to oxygen-vacancy generation [17–19]. Accumulation of these vacancies can lead to the eventual formation of a conductive filament (CF) through the dielectric, which can sustain a large electron current.

The experimental and theoretical results demonstrate that CF formation in m-HfO_2 can proceed via aggregation of O vacancies at grain boundaries [13,20–22]. However, the calculated barriers for vacancy diffusion in the bulk of m-HfO_2 are quite high: 2.38 and 0.69 eV for neutral and doubly positively charged vacancies, respectively [23], for this process to be efficient. On the other hand, diffusion of interstitial oxygen atoms and ions in m-HfO_2 is fast, with activation barriers of the order of 0.5 eV [24]. Therefore, an alternative or complementary scenario can be that oxygen-deficient regions are formed as a result of formation of pairs of Frenkel defects (FDs)—O vacancies and O interstitial atoms or ions near preexisting vacancies accompanied by O interstitial out-diffusion rather than O-vacancy diffusion and aggregation. However, the formation energy of a three-coordinated (3C) and four-coordinated (4C) neutral O vacancy is high, 6.6 and 6.5 eV, respectively [25], and the FD pair formation energy is even higher for charged defects. The question is which factors could aid the generation of additional oxygen vacancies, and what is the mechanism of this process?

It is often assumed that new oxygen vacancy or ion pairs are generated in oxide as a result of stress application where strong electric field weakens Hf—O bonds [14,26]. We investigate whether this process can be aided by electron injection into oxide, particularly at preexisting O vacancies. In metal-insulator-metal RRAM structures, the Fermi level is determined by metal electrodes (TiN, Pt), and, at positive bias, an electron injection from electrodes into the oxide

can proceed via defect states in the gap or Fowler-Nordheim tunneling. It is well established that positively charged and even neutral oxygen vacancies in m-HfO_2 have large affinities to electrons from the conduction band, and neutral vacancies can trap up to two extra electrons, forming negatively charged vacancies [27,28]. It has been shown theoretically that shallow electron polarons can be also formed in m-HfO_2 [29]. In both cases, extra electrons are localized on Hf ions. We study the thermodynamic stability of FD pairs in m-HfO_2 assuming that up to two electrons are injected into the simulation cell from a metal electrode and demonstrate that these extra electrons can weaken Hf—O bonds and reduce energies and barriers for formation of FD pairs.

The results demonstrate that stable oxygen vacancies and charged interstitial oxygen ions can be generated in m-HfO_2 under conditions of electron injection even at zero bias. Extra electrons neutralize a positively charged V^{2+} oxygen vacancy, thus, preventing its recombination with the O^{2-} interstitial oxygen in the FD pair. The O^{2-} interstitial ion can then diffuse away with a (0.5–0.7)-eV activation barrier. The barrier of 2.0 eV to Frenkel pair formation by this mechanism is shown to be lowered down to 1.25 eV by forming a defect pair next to a preexisting neutral oxygen vacancy. Bias application may further lower the barriers for FD pair formation.

II. METHODS OF CALCULATION

Density-functional-theory (DFT) calculations are carried out using the projector-augmented-wave method as implemented in the Vienna *ab initio* simulation package [30,31] and using the Perdew-Wang 91 generalized gradient approximation (GGA) functional [32,33]. To optimize the geometries of the Frenkel pairs a (322–324)-atom, $3\times3\times3$ supercell of monoclinic HfO_2 is used. All calculations are carried out in the Γ point. Defect geometries are relaxed using the conjugate-gradient algorithm to attain forces on ions of less than 0.06 eV $Å^{-1}$. The electronic structure of the FD pair is calculated using the hybrid functional HSE06 [34]. Because of the computational cost of these calculations, a smaller 96-atom, $2\times2\times2$ supercell is used.

Defect formation barriers and barriers to diffusion are calculated using the nudged-elastic-band (NEB) method using eight images and a spring constant of -5.0 eV $Å^{-2}$ [35].

Defect-formation energies $E_{\rm for}(D)$ are calculated using

$$E_{\rm for}(D) = E_D^q - (E_{\rm ref}^q \pm nE_{\rm O}), \qquad (1)$$

where E_D^q is the total energy of the relaxed defective supercell, $E_{\rm ref}^q$ is the energy of the reference cell, n is the number of oxygen atoms added to or removed from the reference cell by production of the defect, and $E_{\rm O}$ is the energy of half an oxygen molecule calculated in an asymmetric unit cell; q is the charge of the periodic cell in the calculation. The Fermi-level position is assumed to be such that extra electrons can be injected into the HfO_2 conduction band, and the formation energy is calculated with respect to perfect cells with no, one, or two electrons at the bottom of the conduction band.

The most stable phase of hafnia is monoclinic and has alternating layers of 3C and 4C oxygen ions. We obtain lattice parameters of the fully optimized structure ($a = 5.136$ Å, $b = 5.193$ Å, $c = 5.317$ Å, and $\gamma = 99.63°$ with PW91 and $a = 5.098$ Å, $b = 5.159$ Å, $c = 5.268$ Å, and $\gamma = 99.39°$ with HSE06) to within 1% of experiment. A Lany-Zunger correction based on an anisotropic point charge is also applied to remove the spurious interactions between the charged defects and their periodic images [36,37].

III. RESULTS OF CALCULATIONS

A. Diffusion of interstitial O ions

Before considering FD pairs, we reevaluate the results of previous calculations of O atom and ion diffusion in m-HfO_2 performed using the GGA PW91 density functional [24]. We use a much bigger 325-atom periodic cell and extend the number of possible diffusion directions in the lattice with respect to Ref. [24]. Interstitial oxygen formation energies are also calculated using the hybrid HSE06 functional in a 96-atom periodic cell.

The formation energies and O—O nearest-neighbor (NN) distances of neutral interstitial O atoms in m-HfO_2 calculated using these two functionals are shown in Table I. Three charge states of oxygen interstitial can be found within the 3C oxygen sublattice dependent on the Fermi-level position [38]. The O—O NN distance increases depending on the charge state of the interstitial ion. In the neutral case, the oxygen ions are close, with an O—O distance of 1.5 Å. This is about 0.3 Å longer than in a free O_2 molecule. At high-Fermi-level position, the interstitial oxygen can trap one or two extra electrons and moves farther away from the lattice oxygen as the bond order is reduced. In the singly charged state, the O—O distance increases to 2.01 Å. In the doubly charged state, the interstitial oxygen becomes a closed-shell ion and has

TABLE I. Formation energies (eV) and nearest-neighbor O—O distances (Å) of interstitial O atoms in m-HfO_2 calculated using the GGA [38] and hybrid density-functional HSE06 in a 96-atom periodic cell.

	PW91		HSE06	
	$E_{{\rm for},D}$	$d_{\rm O—O}$	$E_{{\rm for},D}$	$d_{\rm O—O}$
3C	1.69	1.50	2.00	1.48
4C	2.56	1.50	2.76	1.41

the same Mulliken charge as the lattice oxygens, so it separates until it is around 2.4 Å away from both its oxygen NNs. The O—O distance can, therefore, be used as a good indicator of the charge state of the interstitial ion.

Within the 4C oxygen sublattice, only the neutral oxygen interstitial is stable. This neutral 4C interstitial oxygen, like in the 3C case, has a distance with the nearest lattice O of about 1.5 Å. The 4C O_{int}^{-} and O_{int}^{2-} are unstable, and any attempt to optimize their structures results in the oxygen ions moving into 3C charged interstitial positions. This is due to the closer packing of the O ions in the 4C sublattice, meaning that when the electron localizes on the interstitial oxygen ion and the O—O bond lengthens, there is not sufficient space for the larger interstitial ion to relax into within that sublattice.

The diffusion barriers of the neutral, singly, and doubly negatively charged oxygen interstitials are calculated using GGA in the 325-atom periodic cell and a NEB method. The barrier energies are 0.87, 0.37 and 0.51 eV for the O_{int}^{0}, O_{int}^{-}, and O_{int}^{2-}, respectively. Despite using a larger unit cell, the results are in excellent agreement with Foster *et al.* [24] and follow the same interstitialcy mechanism. To check the effect of using a hybrid functional, O_{int}^{2-} diffusion within the 3C sublattice is also calculated using HSE06 where we find a very similar barrier energy of 0.49 eV.

In each case, the barrier point occurs when the interstitial oxygen is almost equidistant between the lattice oxygen ions in the diffusion pathway. The neutral interstitial has the highest barrier for diffusion and involves the breaking and remaking of the O—O bond. In the 1− case, the electron is fully localized onto the interstitial ion. The interstitial can then move away from its oxygen nearest neighbor than in the neutral case, and the O—O bond is lengthened.

In the 2− case, the interstitial ion maintains an even distance of around 2.4 Å with the nearest oxygen neighbors throughout the diffusion process. Because of the larger Coulomb interaction introduced by the second electron, the lattice displacements around the ion are slightly larger than in the singly charged case, which accounts for the 0.1-eV rise in the barrier energy with respect to the 1− case.

The diffusion barrier for O_{int}^{0} moving between the 3C and 4C sublattices is also calculated at 1.43 eV. The neutral oxygen follows a similar pathway to the 3C case above; however, the distortions through the closer packed 4C sublattice are larger.

B. Formation of nearest-neighbor FD pair

We first consider the FD pair formation in the perfect *m*-HfO_2 lattice using a neutral 324-atom periodic cell and GGA. Starting with the stable O interstitial atom structures, we remove oxygen atoms from different nearest-neighbor oxygen sites to form a NN FD pair. The Fermi-level position in these calculations is at the top of the HfO_2 valence band. Vacancy positions in both the 3C and 4C sublattice are considered. However, since the charged interstitial is unstable in the 4C sublattice, only interstitial positions in the 3C sublattice are considered. The results of FD calculations are summarized in Table II.

TABLE II. Formation energies and adiabatic barriers for formation and recombination of FD pairs (eV). $E_{for,D}$ corresponds to NN FD pair formation energy, $E_{bar,f}$ corresponds to the barrier energy for FD pair formation, and $E_{bar,r}$ the barrier energy for recombination.

n_{elec}	Defect	$E_{for,D}$	$E_{bar,f}$	$E_{bar,r}$
0	$V_3 + O_{int}$	Unstable		
1	$[V_3 + O_{int}]^{-}$	Unstable		
2	$V_3^0 + O_{int}^{2-}$	1.19	1.96	0.77
2	$V_4^0 + O_{int}^{2-}$	2.16	2.64	0.48
0	$2V_3 + O_{int}$	Unstable		
1	$[2V_3 + O_{int}]^{-}$	Unstable		
2	$[2V_3]^0 + O_{int}^{2-}$	0.96	1.25	0.29
3	$[2V_3]^{-} + O_{int}^{2-}$	0.71	1.23	0.52
4	$[2V_3]^{2-} + O_{int}^{2-}$	0.29	1.12	0.83

Removing an O atom creates a neutral O vacancy, which donates two electrons to the interstitial O atom creating a pair of charged defects, e.g., $[V_3^{2+} + O_{int}^{2-}]$. Therefore, in every case the nearest-neighbor FD pairs recombine restoring the perfect lattice caused by a strong Coulomb attraction between the two defects.

We then assume that the Fermi level is at the bottom of the HfO_2 conduction band, and extra electrons are injected in *m*-HfO_2 from an electrode and propagate in the conduction band or form polarons. Thermally activated formation of FD pairs can take place as a result of thermal fluctuations and displacement of an O ion from its site into interstitial position [39]. When one extra electron is trapped, a V^{1+} vacancy is formed. However, the NN FD pair $[V_3^{1+} + O_{int}^{2-}]$ is unstable and recombines. Adding two extra electrons to the system, however, creates a stable NN FD pair because the vacancy is now neutralized by the extra electrons. Therefore, there is no Coulomb attraction between the vacancy and the interstitial O ion, and they remain stable. The distance between the interstitial O and the nearest-neighbor O ions is 2.45 Å, indicating that this is O_{int}^{2-}.

The formation energy for the $[V_3^0 + O_{int}^{2-}]$ pair calculated as the energy difference between the perfect periodic cell with two extra electrons in the conduction band and the final FD pair state is particularly low at 1.19 eV. This low energy results from the energy gained through localizing the two electrons from the HfO_2 conduction band into the positively charged oxygen vacancy. However, the $[V_4^0 + O_{int}^{2-}]$ formation energy is 0.97 eV higher, indicating that the structure of the defect must have a significant impact on the overall formation energy.

The density of states of the FD pair calculated using HSE06 shows an interstitial state 0.1 eV above the

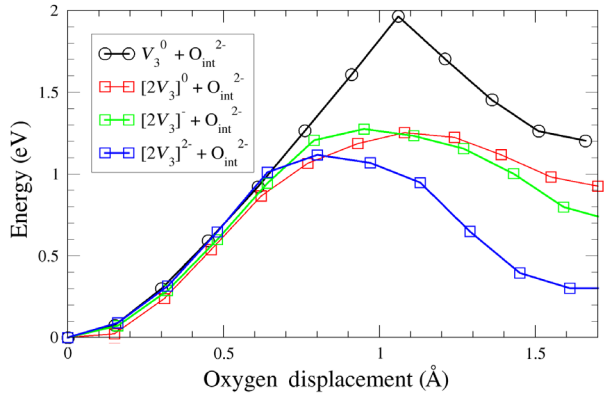

FIG. 1. Barriers of formation for the HfO_2 NN FD pair, divacancy NN FD pair, and charged divacancy NN FD pairs.

valence-band maximum (VBM) and a vacancy state 3.0 and 3.2 eV above the VBM for the 3C and 4C neutral vacancies, respectively, in good agreement with previous calculations [28,38,40]. Formation energies for 4C and 3C NN FD pairs calculated using HSE06 in a 96-atom cell are by about 0.3 eV lower than those calculated using GGA. This reflects the fact that the HfO_2 band gap calculated using HSE06 is wider, and the defect level is lower with respect to the bottom of the conduction band.

The barriers for formation of these defect pairs are calculated using GGA and the NEB method in a 324-atom cell (see Table II). The barrier for the 3C FD pair is significantly lower than for the 4C FD pair. The barriers for formation and recombination of the NN FD pair are shown in Fig. 1. The recombination barrier for the $[V_3^0 + O_{int}^{2-}]$ pair is about 0.8 eV, which is much higher than the O_{int}^{2-} diffusion barrier of 0.5 eV, suggesting that the defects can efficiently separate via O_{int}^{2-} diffusion.

The mechanism of formation of this FD pair corresponds to two electrons effectively assisting thermal fluctuations of the O ion [39] and pushing it out of its site into the interstitial position and occupying the vacancy, thus, gaining extra energy with respect to their energy at the bottom of the conduction band. However, the rate of such process in the perfect lattice is low as it requires a correlated action of two electrons, i.e., high current density. Therefore, we consider whether a similar process can take place at a preexisting O vacancy, which can trap two extra electrons and, thus, significantly increase the cross section of such reaction.

C. Formation of FD pair next to a preexisting vacancy

In order to check whether preexisting oxygen vacancies can facilitate the formation of new vacancies, we calculate the formation energy of a NN FD pair consisting of two O vacancies and one interstitial O ion. Beginning with a stable NN FD pair, a second vacancy is created near the existing vacancy. This process is outlined in Fig. 2 and can be described as follows.

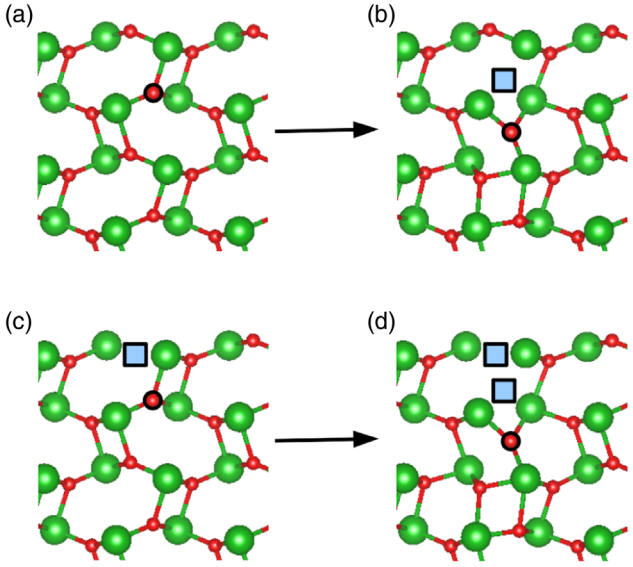

FIG. 2. (a),(b) Formation of a single NN FD pair. (c),(d) Formation of a divacancy NN FD pair in the presence of a preexisting vacancy (large green balls, Hf; small red balls, O; blue squares, vacancy; highlighted red ball, O_{int}^{2-}).

First, we consider a neutral O vacancy in the 323-atom unit cell using the PW91 functional and add two extra electrons. These electrons are delocalized in the conduction band of HfO_2 and do not form a doubly negatively charged O vacancy because the CB is artificially low in the GGA. This state is the starting point, and the energetic reference for further calculations, just as the ideal lattice with two extra electrons is the reference in the NN FD pair calculations.

We then form a second O vacancy near the preexisting one and a nearest-neighbor interstitial O ion by removing an O atom. As in the single-vacancy case above, if none or only one electron are added to the system, an O_{int}^{2-} forms, leaving behind positively charged vacancies. The Coulomb interaction between these charged defects is so large that they recombine during the geometry optimization. However, if two extra electrons are added, the two vacancies are neutralized, and the O_{int}^{2-} ion cannot recombine, creating a stable system of two neutral O vacancies and an interstitial O_{int}^{2-} ion. The cost of forming a $[V_3^0 + O_{int}^{2-}]$ pair next to an existing neutral vacancy is only 0.96 eV. Furthermore, the barrier for the formation of this defect system is calculated to be 1.25 eV, 0.71 eV lower than that for the formation of the NN FD pair from the ideal lattice (see Table II and Fig. 1).

Therefore, the formation of the FD is significantly more likely to occur near a preexisting oxygen vacancy under electron-injection conditions. As one can see in Table II, the addition of more electrons to the cell leads to creation of a charged divacancy and charged interstitial and further lowers the formation energy and the barrier to formation of this defect system.

The barrier profiles for several charge states are summarized in Fig. 1. One can see that the recombination barriers for charged FD pairs are also increasing, reflecting their repulsion. The system of two vacancies and an interstitial O ion is too large to be calculated in the 96-atom cell. Therefore, we are unable to perform HSE06 calculations for this system but can assume that the defect formation energies can be lowered by at least 0.3 eV, as described above.

The results presented above demonstrate an initial trend in forming clusters of O vacancies and charged O_{int} ions at the periphery of the vacancy cluster facilitated by electron injection into the system. The formation energies of these defects are lowered by the additional gain due to the attraction of O vacancies. The binding energies of neutral vacancy aggregates consisting of two, three, and four vacancies have been calculated in Ref. [25]. Generally, these binding energies are found to be small at about 0.2 eV per vacancy, suggesting that there is no strong thermodynamic drive for vacancies to aggregate, but once aggregates are formed, they are reasonably stable. The most stable aggregates have vacancy configurations which form the largest possible void within the bulk m-HfO_2 crystal. This void creates the deepest well for the neutralizing electrons to localize and lowers the overall energy. Importantly, the binding energy per vacancy increases as the aggregate grows, showing that the larger aggregates are more stable. This agrees well with a proposed CF-formation mechanism, which speeds up as the filament grows. Negative divacancies are found to be stable with small binding energies with respect to the neutral cases [25]. This suggests that the formation of an oxygen-deficient region under electron-injection conditions is plausible since vacancy aggregates produced will be stable.

IV. CONCLUSIONS

We use DFT calculations to consider a mechanism by which oxygen vacancies and interstitial ions are formed in m-HfO_2 aided by electron injection. The results demonstrate that such a process is thermodynamically possible in the perfect lattice and near preexisting O vacancies and requires overcoming activation barriers feasible at the temperatures of RRAM electroforming. The preexisting vacancy acts as an electron trap, and the divacancy that forms is stable, further lowering the formation energy of the defect. Furthermore, since the binding energy per vacancy in oxygen-vacancy aggregates increases as the aggregate grows, it is likely that the formation of a NN FD pair next to a larger vacancy aggregate will require even lower formation energy.

Figure 2 shows the proposed vacancy-formation processes. This mechanism requires a concerted action of two electrons. The probability of such process is not high for low electron current densities but increases as the current density increases [41,42]. The fact that this mechanism produces charged O ions is in agreement with voltage-driven ion migration in bipolar devices. Charged interstitial ions are likely to be the fastest diffusing oxygen defect in HfO_2, especially under high positive bias and electron-injection conditions. Such a bias favors neutral and negatively charged vacancies which have diffusion barriers in excess of 2.4 eV [23]. This suggests that effective CF formation in RRAM cells can proceed through creation of new O vacancies in the vicinity of preexisting vacancies, complementary to an aggregation via diffusion processes.

More generally, the results of this work show that the formation of FD pairs in oxides can be aided by electrons in the conduction band. These carriers can be produced by irradiation or tunneling from an electrode. Understanding the electronic mechanisms of defect creation in materials under irradiation and carrier injection is crucial for a wide range of technological applications. Injected electrons can play a significant role in the formation of O-vacancy aggregates and stable oxygen interstitials.

ACKNOWLEDGMENTS

This work is supported by EPSRC. Via our membership of the UK's HPC Materials Chemistry Consortium, which is funded by EPSRC (EP/L000202), this work makes use of the facilities of HECToR and ARCHER, the UK's national high-performance computing service. The work at The Aerospace Corporation was supported by the LTCP program.

[1] Salvatore A. Lombardo, James H. Stathis, and Gennadi Bersuker, The dielectric breakdown in gate oxides under high field stress, ECS Trans. **19**, 177 (2009).

[2] B. Kaczer, R. Degraeve, N. Pangon, and G. Groeseneken, The influence of elevated temperature on degradation and lifetime prediction of thin silicon-dioxide films, IEEE Trans. Electron Devices **47**, 1514 (2000).

[3] X. Li, K. L. Pey, M. Bosman, W. H. Liu, and T. Kauerauf, Direct visualization and in-depth physical study of metal filament formation in percolated high-k dielectrics, Appl. Phys. Lett. **96**, 022903 (2010).

[4] D. J. DiMaria and E. Cartier, Mechanism for stress-induced leakage currents in thin silicon dioxide films, J. Appl. Phys. **78**, 3883 (1995).

[5] Z. Xu, M. Houssa, R. Carter, M. Naili, S. De Gendt, and M. Heyns, Constant voltage stress induced degradation in HfO_2/SiO_2 gate dielectric stacks, J. Appl. Phys. **91**, 10127 (2002).

[6] S. Chatterjee, Y. Kuo, J. Lu, J.-Y. Tewg, and P. Majhi, Electrical reliability aspects of HfO_2 high-k gate dielectrics with TaN metal gate electrodes under constant voltage stress, Microelectron. Reliab. **46**, 69 (2006).

[7] N. A. Chowdhury, D. Misra, G. Bersuker, C. Young, and R. Choi, Role of interfacial layer on breakdown of TiN/high-k gate stacks, J. Electrochem. Soc. **154**, G298 (2007).

[8] D. P. Ioannou, S. Mittl, and G. La Rosa, Positive bias temperature instability effects in nMOSFETs with HfO_2/TiN gate stacks, IEEE Trans. Device Mater. Reliab. **9**, 128 (2009).

[9] D. Veksler, G. Bersuker, M. B. Watkins, and A. L. Shluger, in *Proceedings of the 2014 IEEE International Reliability Physics Symposium, 2014* (IEEE, New York, 2014), pp. 5B.3.1–5B.3.7.

[10] S. Kar, *High Permittivity Gate Dielectric Materials*, Springer Series in Advanced Microelectronics (Springer, Berlin, 2013), p. 489.

[11] M. Houssa, *High-k Gate Dielectrics*, Series in Material Science and Engineering (Taylor & Francis, London, 2003).

[12] T. Grasser, *Bias Temperature Instability for Devices and Circuits* (Springer, New York, 2013).

[13] G. Bersuker, D. C. Gilmer, D. Veksler, P. Kirsch, L. Vandelli, A. Padovani, L. Larcher, K. McKenna, A. Shluger, V. Iglesias, M. Porti, and M. Nafría, Metal oxide resistive memory switching mechanism based on conductive filament properties, J. Appl. Phys. **110**, 124518 (2011).

[14] A. Padovani, L. Larcher, O. Pirrotta, L. Vandelli, and G. Bersuker, Microscopic modeling of HfOx RRAM operations: From forming to switching, IEEE Trans. Electron Devices **62**, 1998 (2015).

[15] F. Nardi, S. Larentis, S. Balatti, D. C. Gilmer, and D. Ielmini, Resistive switching by voltage-driven ion migration in bipolar RRAM 2014; Part i: Experimental study, IEEE Trans. Electron Devices **59**, 2461 (2012).

[16] M. Lanza, A review on resistive switching in high-*k* dielectrics: A nanoscale point of view using conductive atomic force microscope, Materials **7**, 2155 (2014).

[17] B. Traore, P. Blaise, E. Vianello, E. Jalaguier, G. Molas, J. F. Nodin, L. Perniola, B. De Salvo, and Y. Nishi, in *Proceedings of the 2014 IEEE International Reliability Physics Symposium, 2014* (IEEE, New York, 2014), pp. 5E.2.1–5E.2.5.

[18] L. Goux, P. Czarnecki, Y. Y. Chen, L. Pantisano, X. P. Wang, R. Degraeve, B. Govoreanu, M. Jurczak, D. J. Wouters, and L. Altimime, Evidences of oxygen-mediated resistive-switching mechanism in TiN/HfO_2/Pt cells, Appl. Phys. Lett. **97**, 243509 (2010).

[19] L. Goux, N. Raghavan, A. Fantini, R. Nigon, S. Strangio, R. Degraeve, G. Kar, Y. Y. Chen, F. De Stefano, V. V. Afanas'ev, and M. Jurczak, On the bipolar resistive-switching characteristics of Al_2O_3 and HfO_2-based memory cells operated in the soft-breakdown regime, J. Appl. Phys. **116**, 134502 (2014).

[20] K. McKenna and A. Shluger, The interaction of oxygen vacancies with grain boundaries in monoclinic HfO_2, Appl. Phys. Lett. **95**, 222111 (2009).

[21] K. Shubhakar, K. L. Pey, N. Raghavan, S. S. Kushvaha, M. Bosman, Z. Wang, and S. J. O'Shea, Study of preferential localized degradation and breakdown of HfO_2/SiO_x dielectric stacks at grain boundary sites of polycrystalline HfO_2 dielectrics, Microelectron. Eng. **109**, 364 (2013).

[22] M. Lanza, K. Zhang, M. Porti, M. Nafría, Z. Y. Shen, L. F. Liu, J. F. Kang, D. Gilmer, and G. Bersuker, Grain boundaries as preferential sites for resistive switching in the HfO_2 resistive random access memory structures, Appl. Phys. Lett. **100**, 123508 (2012).

[23] N. Capron, P. Broqvist, and A. Pasquarello, Migration of oxygen vacancy in HfO_2 and across the HfO_2/SiO_2 interface: A first-principles investigation, Appl. Phys. Lett. **91**, 192905 (2007).

[24] A. S. Foster, A. L. Shluger, and R. M. Nieminen, Mechanism of Interstitial Oxygen Diffusion in Hafnia, Phys. Rev. Lett. **89**, 225901 (2002).

[25] S. R. Bradley, G. Bersuker, and A. L. Shluger, Modelling of oxygen vacancy aggregates in monoclinic HfO_2: Can they contribute to conductive filament formation?, J. Phys. Condens. Matter **27**, 415401 (2015).

[26] J. McPherson, J.-Y. Kim, A. Shanware, and H. Mogul, Thermochemical description of dielectric breakdown in high dielectric constant materials, Appl. Phys. Lett. **82**, 2121 (2003).

[27] J. L. Gavartin, D. Muñoz Ramo, A. L. Shluger, G. Bersuker, and B. H. Lee, Negative oxygen vacancies in HfO_2 as charge traps in high-*k* stacks, Appl. Phys. Lett. **89**, 082908 (2006).

[28] P. Broqvist and A. Pasquarello, Oxygen vacancy in monoclinic HfO_2: A consistent interpretation of trap assisted conduction, direct electron injection, and optical absorption experiments, Appl. Phys. Lett. **89**, 262904 (2006).

[29] J. L. Gavartin, D. Muñoz Ramo, A. L. Shluger, and G. Bersuker, Polaron-like charge trapping in oxygen deficient and disordered HfO_2: Theoretical insight, ECS Trans. **3**, 277 (2006).

[30] G. Kresse and J. Furthmüller, Efficient iterative schemes for *ab initio* total-energy calculations using a plane-wave basis set, Phys. Rev. B **54**, 11169 (1996).

[31] G. Kresse and J. Furthmüller, Efficiency of ab-initio total energy calculations for metals and semiconductors using a plane-wave basis set, Comput. Mater. Sci. **6**, 15 (1996).

[32] J. P. Perdew, J. A. Chevary, S. H. Vosko, K. A. Jackson, M. R. Pederson, D. J. Singh, and C. Fiolhais, Atoms, molecules, solids, and surfaces: Applications of the generalized gradient approximation for exchange and correlation, Phys. Rev. B **46**, 6671 (1992).

[33] J. P. Perdew, J. A. Chevary, S. H. Vosko, K. A. Jackson, M. R. Pederson, D. J. Singh, and C. Fiolhais, Erratum: Atoms, molecules, solids, and surfaces: Applications of the generalized gradient approximation for exchange and correlation, Phys. Rev. B **48**, 4978 (1993).

[34] A. V. Krukau, O. A. Vydrov, A. F. Izmaylov, and G. E. Scuseria, Influence of the exchange screening parameter on the performance of screened hybrid functionals, J. Chem. Phys. **125**, 224106 (2006).

[35] H. Jónsson, G. Mills, and K. W. Jacobsen, *Classical and Quantum Dynamics in Condensed Phase Simulations* (World Scientific, Singapore, 1998), Chap. 16, pp. 385–404.

[36] S. Lany and A. Zunger, Assessment of correction methods for the band-gap problem and for finite-size effects in supercell defect calculations: Case studies for ZnO and GaAs, Phys. Rev. B **78**, 235104 (2008).

[37] S. T. Murphy and N. D. M. Hine, Anisotropic charge screening and supercell size convergence of defect formation energies, Phys. Rev. B **87**, 094111 (2013).

[38] A. S. Foster, F. Lopez Gejo, A. L. Shluger, and R. M. Nieminen, Vacancy and interstitial defects in hafnia, Phys. Rev. B **65**, 174117 (2002).

[39] J. L. Gavartin and A. L. Shluger, Thermal fluctuations, localization, and self-trapping in a polar crystal: Combined shell-model molecular dynamics and quantum chemical approach, Phys. Rev. B **64**, 245111 (2001).

[40] K. Xiong, J. Robertson, M. C. Gibson, and S. J. Clark, Defect energy levels in HfO_2 high-dielectric-constant gate oxide, Appl. Phys. Lett. **87**, 183505 (2005).

[41] P. N. Murgatroyd, Theory of space-charge-limited current enhanced by Frenkel effect, J. Phys. D **3**, 151 (1970).

[42] A. Rose, Space-charge-limited currents in solids, Phys. Rev. **97**, 1538 (1955).